Surface functionalization of carbon nanotubes by direct encapsulation with varying dosages of amphiphilic block copolymers

2015 Nanotechnology 26 325601

(http://iopscience.iop.org/0957-4484/26/32/325601)

IOP Publishing Nanotechnology
Nanotechnology **26** (2015) 325601 (10pp) doi:10.1088/0957-4484/26/32/325601

Surface functionalization of carbon nanotubes by direct encapsulation with varying dosages of amphiphilic block copolymers

Xueping Yao, Jie Li, Liang Kong and Yong Wang

State Key Laboratory of Materials-Oriented Chemical Engineering, College of Chemical Engineering, Nanjing Tech University, Nanjing 210009, Jiangsu, People's Republic of China

E-mail: yongwang@njtech.edu.cn

Received 23 April 2015, revised 11 June 2015
Accepted for publication 24 June 2015
Published 23 July 2015

Abstract

Encapsulation of carbon nanotubes (CNTs) by amphiphilic block copolymers is an efficient way to stabilize CNTs in solvents. However, the appropriate dosages of copolymers and the assembled structures are difficult to predict and control because of the insufficient understanding on the encapsulation process. We encapsulate multiwalled CNTs with polystyrene-*block*-poly (4-vinyl pyridine) (PS-*b*-P4VP) by directly mixing them in acetic acid under sonication. The copolymer forms a lamellar structure along the surface of CNTs with the PS blocks anchoring on the tube wall and the P4VP blocks exposed to the outside. The encapsulated CNTs achieve good dispersibility in polar solvents over long periods. To increase our understanding of the encapsulation process we investigate the assembled structures and stability of copolymer/CNTs mixtures with changing mass ratios. Stable dispersions are obtained at high mass ratios between the copolymer and CNTs, i.e. 2 or 3, with the presence of free spherical micelles. Transmission electron microscopy and thermal gravimetric analysis determine that the threshold for the complete coverage of CNTs by the copolymer occurs at the mass ratio of 1.5. The coated copolymer layer activates the surface of CNTs, enabling further functionalization of CNTs. For instance, atomic layer deposition of TiO_2 produces conformal thin layers on the encapsulated CNTs while isolated TiO_2 bumps are produced on the pristine, inert CNTs.

Keywords: carbon nanotube, amphiphilic block copolymers, functionalization, atomic layer deposition

(Some figures may appear in colour only in the online journal)

1. Introduction

Carbon nanotubes (CNTs) have attracted tremendous interest and have been investigated for applications in diverse fields due to their superior mechanical strength, electrical conductivity, thermal stability, chemical resistance, etc [1–3]. However, despite these remarkable features of CNTs, their potential application in many fields, e.g. composite materials, is frequently hindered by their low solubility and poor dispersion in solvents. As-synthesized CNTs are prone to aggregate into insoluble bundles or randomly stacked networks due to the van der Waals interaction between the tube walls. To address such issues and to tune their properties, various methods have been utilized for dispersing bundled or networked CNTs into individual nanotubes by high-energy sonication, covalent and noncovalent modifications to the surface of CNTs [4–6]. In addition, simulation works have also been done to explore the interactions between CNTs and polymers. For example, Ruckenstein and coworkers employed molecular dynamics simulations and dissipative particle dynamics simulations to investigate the phase behavior between CNT-like particles and polymers [7–9].

Covalent modifications typically generate unwanted tube defects upon the destruction of the continuous π-electronic structure, thus jeopardizing their intrinsic electronic and mechanical properties. Alternatively, the noncovalent adsorption of either low-molecular-weight surfactants [10] or bulky polymeric chains [11–13] onto tube walls has been applied as a mild and effective approach for the dispersion of CNTs; this approach maintains the pristine structure of CNTs to the largest extent.

Among different types of polymeric dispersants to CNTs, block copolymers (BCPs) are unique and have received particular interest because of their great flexibility in molecular architecture design and the consequent tunability in the functionality of the coated CNTs [13–15]. BCPs are composed of two or more chemically distinct homopolymer chains which are covalently linked together. To serve as an effective dispersant to CNTs, BCPs should contain at least one block having specific interactions to tube walls [16, 17]. Amphiphilic BCPs containing both hydrophobic blocks and more hydrophilic blocks are frequently used. Typical examples include triblock copolymers of polyethylene oxide-*block*-polypropylene oxide-*block*-polyethylene oxide (PEO-*b*-PPO-*b*-PEO) [18, 19], and diblock copolymers of polystyrene-*block*-polyacrylic acid (PS-*b*-PAA) [20–22], and polystyrene-*block*-poly(2 or 4-vinyl pyridine) (PS-*b*-P2VP, PS-*b*-P4VP) [23–25], etc. However, most works simply use significantly excessive BCPs to ensure the complete coverage of BCPs on CNTs and sufficient dispersibility because of the insufficient understanding on the coating process of BCPs on CNTs. Overdosed BCPs produce undesired byproducts, typically micelles, which are mixed with the BCP-coated CNTs. The byproducts waste BCPs and even worse, they contaminate the coated CNTs and would bring adverse effects in the applications of the coated CNTs. Tedious efforts are needed to purify the coated CNTs by removing these byproducts from the mixture. For example, Taton *et al* coated single-walled CNTs by PS-*b*-PAA and empty micelles without CNTs were also produced. They had to use three or more consecutive cycles of centrifugation to remove the empty micelles from the coated CNTs [20]. Therefore, it is highly desired to have a detailed understanding on the encapsulation process of CNTs by BCPs and to obtain the threshold point for the complete coverage of CNTs with BCP molecules, which allows us not only to produce dispersible CNTs with high purity by eliminating the formation of the byproducts but also to use BCPs in a more economical way. In this work, we study the direct encapsulation of multiwalled CNTs by poly(styrene)-*block*-poly(4-vinylpyridine) (hereafter denoted as S4VP) with an emphasis on the detailed investigation of the threshold of the encapsulation, which is helpful for an in-depth understanding on the encapsulation process as well as for the formulation of CNT-involved nanocomposites. In addition, we demonstrate that the coated S4VP layers modulated the atomic layer deposition of TiO_2 on CNTs.

2. Experiment

2.1. Materials

Block copolymer of S4VP (M_n(PS) = 12000 g mol^{-1}, M_n(P4VP) = 1700 g mol^{-1}, M_w/M_n = 1.09), was purchased from Polymer Source Inc. and used as received. CNTs (outside diameter: 10 ± 1 nm, inside diameter: 4.5 ± 0.5 nm, length: 3–6 μm) with purity higher than 98% were obtained from Sigma-Aldrich and used without any pretreatment. Titanium isopropylate (TIP) with a purity of 98% used as the precursor for the ALD of TiO_2 was purchased from Aladdin Reagents. Acetic acid (AA) and ethanol with purity ⩾99.5% were obtained from local suppliers.

2.2. Encapsulation of CNTs by S4VP

We mixed CNTs and S4VP at three different mass ratios. First, 5 mg of CNTs were added into 10 g of AA and sonicated for 30 min at the power of 350 W. Then 5, 10, or 15 mg of S4VP were added into the CNTs previously suspended in AA and sonicated for another 2 h at the power of 100 W, thus obtaining S4VP/CNTs in AA mixtures with the mass ratio between BCP and CNTs (m_{BCP}/m_{CNT}) of 1, 2, and 3, respectively. The prepared S4VP/CNTs mixtures were diluted with ethanol or water for different folds, if necessary.

2.3. Atomic layer deposition of TiO_2 on pristine CNTs and S4VP-coated CNTs

For the ALD of TiO_2, the ethanolic suspensions of pristine CNTs and S4VP-coated CNTs were separately deposited on carbon-coated copper grids and dried at 40 °C for 2 h to evaporate the solvent. The deposition was performed in an ALD reactor (Savannah 100, Cambridge) at 80 °C under the pressure <2 torr and nitrogen was used as both the carrier and purge gas at the flow rate of 20 sccm. Deionized water and TIP were used as the precursors. In a typical ALD cycle, the pulse time for TIP and water was 0.03 s and 0.015 s, respectively, and for both precursors, the exposure and purge time were 5 s and 30 s, respectively. Both the pristine and S4VP-coated CNTs were subjected to TiO_2 ALD for 100 cycles.

2.4. Characterizations

Transmission electron spectroscopy (TEM) was conducted on a JEM-2100 microscope (JEOL) operated at 200 kV or G2 F30 S-TWIN microscope (Tecnai) operated at 300 kV. The samples in liquid suspensions were prepared by depositing droplets of the suspension onto lacey carbon copper grids, allowing the grids to dry at the temperature of 40 °C for 3 h. The ALD-deposited samples were already supported on copper grids and they were used for TEM examination directly after deposition. Thermal gravimetric analysis (TGA) was performed in nitrogen on a TG209F1 thermal analyzer (NETZSCH) with a heating rate of 10 °C min^{-1}. Before the TGA tests, the S4VP/CNTs mixture was pre-filtered by a PVDF membrane with a nominal pore diameter of 0.22 μm to

eliminate the S4VP micelles coexisting with the coated CNTs. Raman spectroscopy was measured on an HR800 Raman spectrometer (Horiba) using the excitation laser with the wavelength of 514 nm and the spectral resolution of 1.7 cm^{-1}. The absorbance of S4VP-coated CNTs mixtures with different dilution rates was obtained from a NanoDROP 2000C UV–Vis spectrometer (Thermo Scientific). X-ray photoelectron spectroscopy (XPS) was carried out on an ESCALAB 250 XPS system (Thermo Scientific) employing a monochromatic Al K_α x-ray source. The samples were prepared by drop-casting of S4VP in chloroform solution and S4VP-coated CNTs in ethanol suspension onto silicon substrates, followed by drying at the temperature of 40 °C for 2 h.

3. Results and discussions

3.1. Dispersion of CNTs in polar solvents with the assistance of S4VP

Pristine CNTs cannot be directly dispersed in polar solvents like AA even under strong sonication for hours because of the strong intertube interactions. As shown in figure 1(a), pristine CNTs added into AA started to precipitate immediately after terminating sonication. Introduction of the amphiphilic block copolymer of S4VP improved the dispersibility of CNTs in AA and the improvement was dependent on the dosage of S4VP, or in other words, the mass ratio of S4VP and CNTs, m_{BCP}/m_{CNT}. At $m_{BCP}/m_{CNT} = 1$ CNTs were suspended in AA as large aggregates. At higher values of m_{BCP}/m_{CNT}, for instance, 2 or 3, CNTs were homogeneously dispersed in AA and remained stable for more than six months when stored at room temperature.

With the presence of adequate of S4VP, CNTs exhibited good dispersion in polar solvents and can be diluted with many solvents including ethanol and water without losing their dispersibility. We diluted the S4VP/CNTs in the AA mixture with $m_{BCP}/m_{CNT} = 2$ with ethanol by 15–50 times and examined their dispersion by monitoring the change of their absorption. The same concentration of the S4VP solution was used as reference to eliminate the absorbance of S4VP in the mixture. A calibration line that correlates the solution absorbance at the wavelength of 500 nm as a function of the relative concentration of the S4VP/CNTs mixture was linearly fitted (figure 1(b)), which implies that CNTs are well dispersed and stabilized in AA with the presence of the suited amount of S4VP. Figure 1(c) displays the absorbance of the S4VP/CNTs mixtures with different dilution folds after storing for different periods up to 1 month. Comparing to the as-prepared mixture, the absorption intensity barely changed, suggesting the long-term stability of the S4VP/CNTs mixtures with different concentrations.

3.2. Mechanism for the stabilization of CNTs by S4VP

We first used TEM to investigate the morphology of CNTs collected from their mixtures with S4VP in AA. The morphologies of the pristine CNTs and the S4VP-coated CNTs prepared at $m_{BCP}/m_{CNT} = 2$ were characterized and the images with different magnifications are shown in figure 2. It can be clearly seen from figures 2(a) and (b) that the pristine CNTs possess the morphology of hollow tubes and consisted of approximately 10 layers of graphene sheets with the total wall thickness of around 3.0 nm. The average diameter of the entire tubes is reasonably well distributed with an average diameter of 10.9 nm (figure 2(a), inset). With the presence of S4VP at $m_{BCP}/m_{CNT} = 2$ a core/shell composite structure appears and CNTs are judged to be residing in the center of the composite structure as their crystalline lattices remain clearly visible. An amorphous shell is conformally coated along the outer surface of the CNTs. The amorphous shell can only be the S4VP copolymer and it exhibits a very uniform thickness of a few nanometers, forming a complete coating layer along the wall of CNTs. The S4VP-coated CNTs display an integrated outer diameter of 20.2 nm and the thickness of the S4VP shell can be deduced to be 4.7 nm considering that CNTs have a diameter of 10.9 nm. The inset of figure 2(c) demonstrates the relatively narrow diameter distribution of the coated CNTs, confirming the uniform thickness of the S4VP coating layer and the complete coverage of CNTs by S4VP.

From the morphology examination, we understand that the presence of a coating layer of S4VP on the surface of CNTs enables their dispersion and stabilization in polar solvents. The functions of S4VP should be originated from its amphiphilic nature and the two constituent blocks of S4VP are playing different roles. The hydrophobic PS blocks anchor on the surface of CNTs while the relatively hydrophilic P4VP blocks are solvated and extended in polar solvents. Because the two blocks are covalently bonded together the solvated P4VP blocks prevent the entire S4VP-coated CNTs composite structure from aggregation or precipitation. Accordingly, it is expected that the S4VP chains possess a lamellar structure along the surface of CNTs with PS connecting both CNTs and P4VP blocks and P4VP existing as the outermost layer. We tried to observe such a lamellar structure under TEM after staining the S4VP-coated CNTs with iodine, as the structure would be selectively enriched in the P4VP domains [26]. However, as the volume fraction of P4VP is much less than that of PS and the total thickness of the S4VP layer is extremely thin down to 4.7 nm (figure 2(d)), we cannot clearly discern the stained P4VP phase from the composite structure. Alternatively, we used XPS to reveal the preferential segregation of P4VP chains on the outermost surface of the S4VP-coated CNTs. We compare the surface content of nitrogen of a solution-casted S4VP film and the S4VP-coated CNTs. The S4VP film was casted from its solution in chloroform and was believed to have a balanced surface with minimal selective segregation of either block, as chloroform is a good solvent for both the PS and P4VP block [27]. Weak signals of nitrogen appear on the XPS spectrum of both the casted S4VP film and the S4VP-coated CNTs. However, the atomic ratio of N to C (N/C) of the S4VP-coated CNTs is 2.99%, being noticeably higher than that of the casted S4VP film (1.60%). Higher N/C in S4VP-coated CNTs implies that the selective segregation of P4VP chains on the outermost

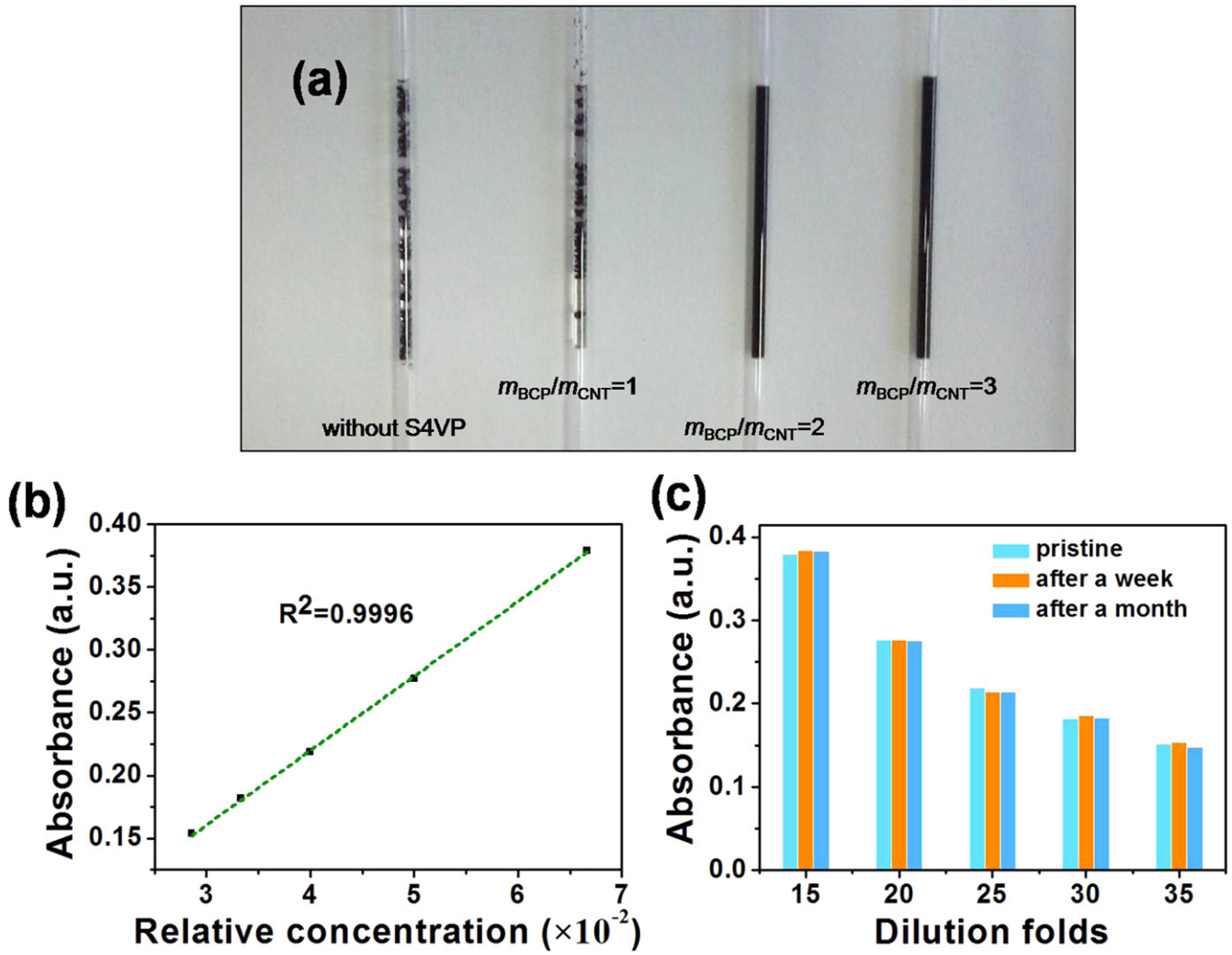

Figure 1. (a) Photographs of CNTs dispersion in AA with different mass ratios between S4VP and CNTs. To have a better view, the mixtures were filled into capillary tubes. (b) Absorption intensity at the wavelength of 500 nm of the S4VP/CNTs mixtures ($m_{BCP}/m_{CNT} = 2$) with different concentrations. The green line is a linear fit the experimental data. (c) The absorbance at the wavelength of 500 nm of the S4VP/CNTs mixtures ($m_{BCP}/m_{CNT} = 2$) with changing dilution times after storage for different periods.

surface of the coated CNTs as nitrogen only exists in the P4VP blocks and its content directly indicates the concentration of P4VP chains.

The PS blocks in S4VP mediate the attachment of S4VP chains on the surface of CNTs through the π-π stacking interaction between the benzyl rings and CNTs, which is confirmed by Raman spectroscopy. As can be seen from figure 3, the Raman spectrum of pristine CNTs is featured with the *G* band locating at 1577 cm^{-1} and the *D* band at 1342 cm^{-1}, corresponding to the graphitic and disordered phases of CNTs, respectively [28]. In the Raman spectrum of the S4VP-coated CNTs, the two bands remain but are evidently shifted to 1590 and 1354 cm^{-1}, respectively. Such a shift in the characteristic bands of CNTs indicates the attachment of polymer chains onto the surface of CNTs and it has been observed that characteristic Raman bands of CNTs will shift to higher frequencies upon being incorporated into a polymeric matrix [29]. The presence of S4VP in the coated CNTs is also evidenced by another band centering around 1106 cm^{-1} which is the characteristic band of S4VP as this band also appears at the same frequency in the spectrum of the pure S4VP. Moreover, no new bands can be discerned in the spectrum of the S4VP-coated CNTs, suggesting that the interaction between CNTs and S4VP is exclusively the π-π stacking-dominated surface interaction.

3.3. The critical m_{BCP}/m_{CNT} for the stabilization of CNTs by S4VP

As mentioned in section 3.1, the quality of dispersion of CNTs in AA is dependent on the dosage of S4VP and a stable dispersion can only be achieved at sufficiently high m_{BCP}/m_{CNT}. Therefore, there should be a threshold for m_{BCP}/m_{CNT} above which there will be free S4VP dissolved in the solution, not coated on CNTs. Actually, we observed the inadequate coverage of S4VP on CNTs at low m_{BCP}/m_{CNT}s. TEM observations on S4VP-coated CNTs prepared at $m_{BCP}/m_{CNT} = 1$ reveals a rough layer of S4VP with a varying thickness up to ~3 nm formed on the CNTs' surface

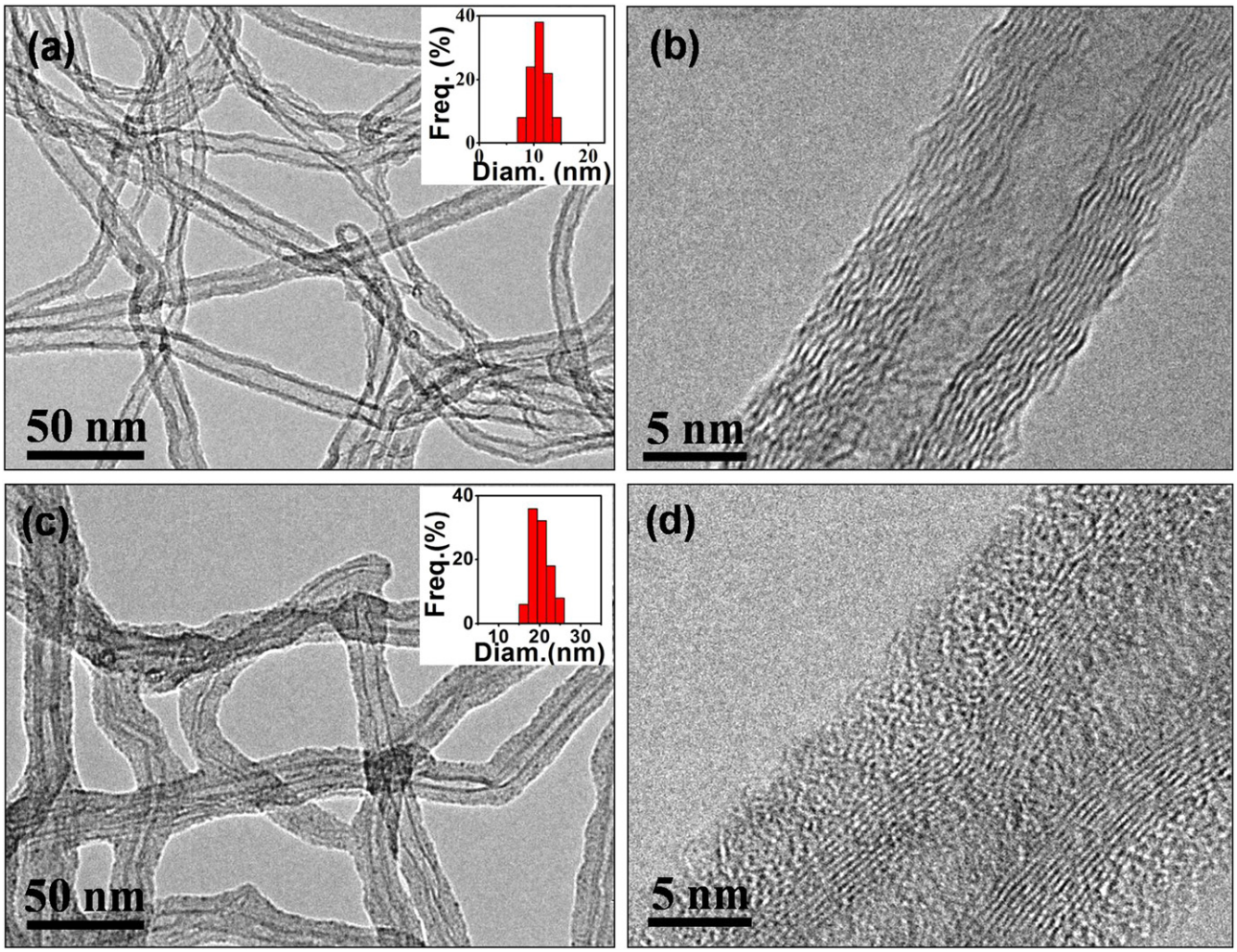

Figure 2. TEM images of the pristine CNTs (a)–(b) and the S4VP-coated CNTs prepared at the m_{BCP}/m_{CNT} of 2 (c)–(d) at different magnifications. Insets shown in (a) and (c) are the profiles of the diameter distribution of the corresponding samples.

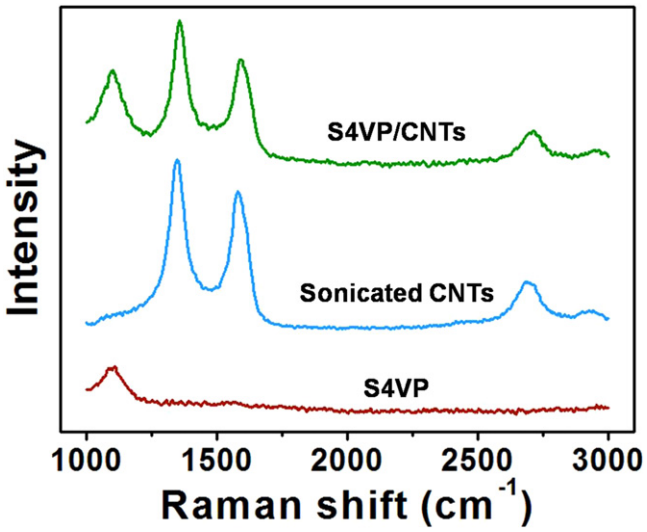

Figure 3. The Raman spectrum of the sonicated CNTs, the pure S4VP, and the S4VP-coated CNTs.

(figure 4(b)). Even worse, there are some positions on the surface of the CNTs on which no S4VP coating layer could be observed, suggesting the incomplete coating of CNTs at low dosages of S4VP (see the arrow in figure 4(b)). Such incompletely coated CNTs precipitated soon from their mixture with AA (for instance, figure 1(a)) because of the inadequate enhancement in the affinity of the coated CNTs toward AA. In contrast, CNTs could be well dispersed and remained stable for a long time in AA if we used higher dosages of S4VP, for example, $m_{BCP}/m_{CNT} = 2$ or 3. As shown in figure 4(c), S4VP forms a uniform coating layer along the surface of CNTs at $m_{BCP}/m_{CNT} = 3$ and the thickness of the coating layer of S4VP remains unchanged compared to that prepared at $m_{BCP}/m_{CNT} = 2$. Interestingly, when $m_{BCP}/m_{CNT} = 3$, there appear many spherical nanoparticles with a diameter of 20 nm in addition to the S4VP-coated CNTs. Such nanoparticles could also be occasionally observed together with S4VP-coated CNTs prepared at $m_{BCP}/m_{CNT} = 2$ and rarely seen at $m_{BCP}/m_{CNT} = 1$. These particles are micelles of the excessive S4VP molecules which do not have the chance to be coated on CNTs. AA is a

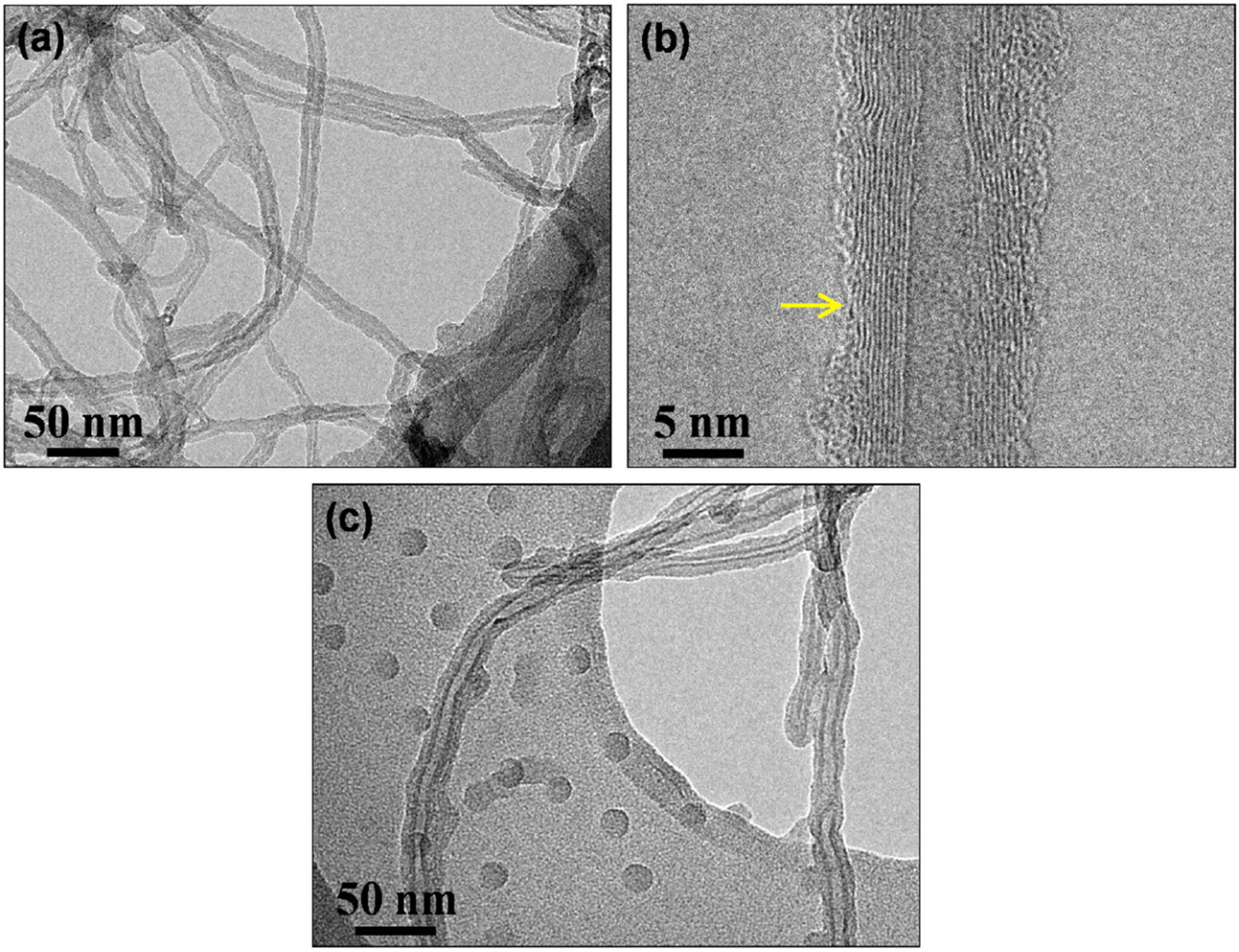

Figure 4. TEM images of the mixture of BCP and CNT at $m_{BCP}/m_{CNT} = 1$ (a), (b) and at $m_{BCP}/m_{CNT} = 3$ (c).

selective solvent to P4VP blocks and micelles are produced following the direct micellization mechanism as the S4VP used in this work has a relatively low molecular weight [30, 31].

By comparing the presence of S4VP micelles and the uniformity of the coated S4VP layers, we can roughly estimate that the threshold of m_{BCP}/m_{CNT} for the complete coating of the surface of CNTs is somewhere between 1 and 2. We performed a detailed analysis on the TEM images of the S4VP-coated CNTs prepared at $m_{BCP}/m_{CNT} = 2$ to obtain a more accurate value for the critical m_{BCP}/m_{CNT}. Based on the data of the wall thickness of CNTs and the thickness of the S4VP shell, we can calculate that the volume ratio of S4VP to CNTs is 3.08. Given that the densities of graphite consisting of walls of CNTs and S4VP are 2.2 g cm^{-3} [32] and 1.05 g cm^{-3} [33], respectively, we know that the mass ratio between S4VP and CNTs is 1.47.

Considering the big difference in the thermal stability of S4VP and CNTs, we used TG analysis to alternatively investigate the mass ratio between S4VP and CNTs of the S4VP-coated CNTs prepared at $m_{BCP}/m_{CNT} = 2$. To avoid the interference of the S4VP micelles in the mixture, the mixture was filtrated through a membrane with a nominal pore size of 0.22 μm to separate the micelles from CNTs and the collected CNTs were then dried and used for TG analysis. As shown in figure 5, the as-received CNTs only slightly lose 1.7% of their weight when heated to 700 °C whereas the CNTs sonicated in AA for hours lose 10.2% of their weight, possibly because sonication in AA produces some structural defects on the surface of CNTs, partially reducing the thermal stability of CNTs. The residual weight percentages of pure S4VP and S4VP-coated CNTs were 0.8% and 36.4 wt%, respectively. It is reasonable to assume that CNTs in the S4VP-coated CNTs composite structure will also experience a ~10% weight loss like the sonicated CNTs when heated to 700 °C. Based on the above data of residual weight percentages of different components in the S4VP-coated CNTs, we can estimate that CNTs account for 40% of the total weight in the composite structures, that is, the mass ratio of S4VP and CNTs is 1.50, which is in very good agreement with the results obtained from TEM analysis.

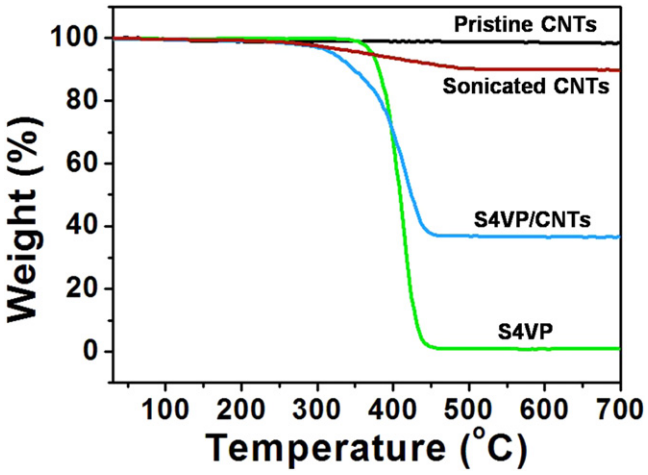

Figure 5. TGA curves of as-received CNTs, sonicated CNTs, pure S4VP, and S4VP-coated CNTs prepared at $m_{BCP}/m_{CNT} = 2$.

3.4. Understanding the encapsulation process of CNTs with S4VP

As the critical m_{BCP}/m_{CNT} is determined to be ~1.5, the mixture of S4VP and CNTs in AA with m_{BCP}/m_{CNT}s higher than this threshold will contain not only S4VP-coated CNTs but also excessive S4VP chains which are not incorporated into the coating S4VP layer on CNTs. These excessive S4VP chains easily aggregate into micelles as the critical micellization concentrations of block copolymers are typically very low [34]. Control tests reveal that mixing S4VP with AA without the presence of CNTs yields spherical micelles displaying the same morphology and diameter with the ones found in the mixture with $m_{BCP}/m_{CNT} = 2$ or 3. At $m_{BCP}/m_{CNT} = 2$, S4VP is moderately overdosed compared to the threshold m_{BCP}/m_{CNT} and therefore we occasionally observed micelles assembled from the excessive S4VP. We note that the presence of these S4VP micelles does not affect the dispersion of CNTs and the micelles themselves are also well-stabilized in AA as they possess condensed PS cores and extended P4VP shells enabling the dispersion of the micelles in AA [31]. At $m_{BCP}/m_{CNT} = 3$ where the dosage of S4VP is far beyond the threshold nearly half of the added S4VP is present as micelles in the mixture and we see many more micelles as their number is much larger than that of the case at $m_{BCP}/m_{CNT} = 2$.

The driving force for the dispersion of CNTs in polar solvents is believed to be the specific interaction between S4VP and CNTs. S4VP is an amphiphilic macromolecule containing both a nonpolar PS block and a comparably polar P4VP block. When mixed with CNTs in AA under sonication, the added S4VP solids would be molecularly dissolved to form unimers as AA will strongly solvate with the P4VP chains (figure 6(a)). S4VP used in this work can be dissolved in AA at room temperature, progressively generating free S4VP unimers at the initial stage. Upon approaching the CNT surface from the side of the PS blocks the S4VP unimers will be arrested by CNTs as there is a strong π-π interaction between CNTs and PS blocks, and the P4VP blocks on the other side of the copolymer remain solvated. The solvated P4VP blocks prohibit the energetically unfavorable contact of the hydrophobic CNTs and PS blocks with the polar solvent of AA, leading to the stabilization of CNTs in the solvent (figure 6(b)). After CNTs have been completely coated by S4VP chains, excessive unimers generated by the continuous dissolution of S4VP solids will assemble with each other to form aggregates, eventually forming spherical micelles with PS chains condensed inside the micelle cores when the S4VP unimers reaches the critical micellization concentration (figure 6(c)).

To confirm the scenario of the encapsulation of CNTs by S4VP discussed above, we first dissolved S4VP in AA to prepare an S4VP micellar solution and then mixed CNTs into the micellar solution with the assistance of sonication for 30 min ($m_{BCP}/m_{CNT} = 2$). CNTs can be well dispersed in the micellar solution and maintained long-term stability. As shown in figure 7, TEM examinations discover that there is also a thin amorphous layer with a thickness of ~2–4 nm along the surface of CNTs. Therefore, the stabilization is also realized by the encapsulation effect of S4VP, similar to the co-dissolution approach we used previously in this work where CNTs and S4VP solids were added into AA simultaneously. After adding into the S4VP micellar solution, CNTs will attract S4VP unimers in the solution because of the strong interaction between the PS blocks and tube walls, leading to the reduction of the concentration of S4VP unimers in the solution. To maintain the equilibrium some S4VP chains are released from the S4VP micelles, eventually resulting in the disassembly of some S4VP micelles. S4VP chains remain adsorbed on the surface of CNTs with the consumption of pre-formed S4VP micelles until the complete coverage of CNTs. Shin and coworkers previously employed S4VP micellar solutions to stabilize single-walled CNTs in ethanol and they attributed the stabilization to the adsorption of entire S4VP micelles on CNTs [19]. This explanation might be true as they used S4VP copolymers with molecular weights different than the ones used in the current work. However, there might also be a S4VP layer conformally coating along the CNTs, enhancing their dispersibility, although their TEM results were not clear enough to discern such layers.

3.5. Modulating the atomic layer deposition of TiO_2 on CNTs

With the presence of polymers coated on CNTs, the surface properties of CNTs are changed accordingly, allowing further functionalization and modification to CNTs independent of the chemistry of the CNTs themselves. As a demonstration for the capability of the coated S4VP layer to tune the surface functionality of CNTs, we showed that thin layers of TiO_2 were able to be deposited on CNTs with S4VP serving as the mediating layer. We performed ALD deposition of TiO_2 on both the pristine and S4VP-coated CNTs for 100 cycles. TEM observations reveal that TiO_2 is deposited on the pristine CNTs as isolated irregular bumps (figure 8(a)) while TiO_2 forms a continuous conformal layer with the thickness of

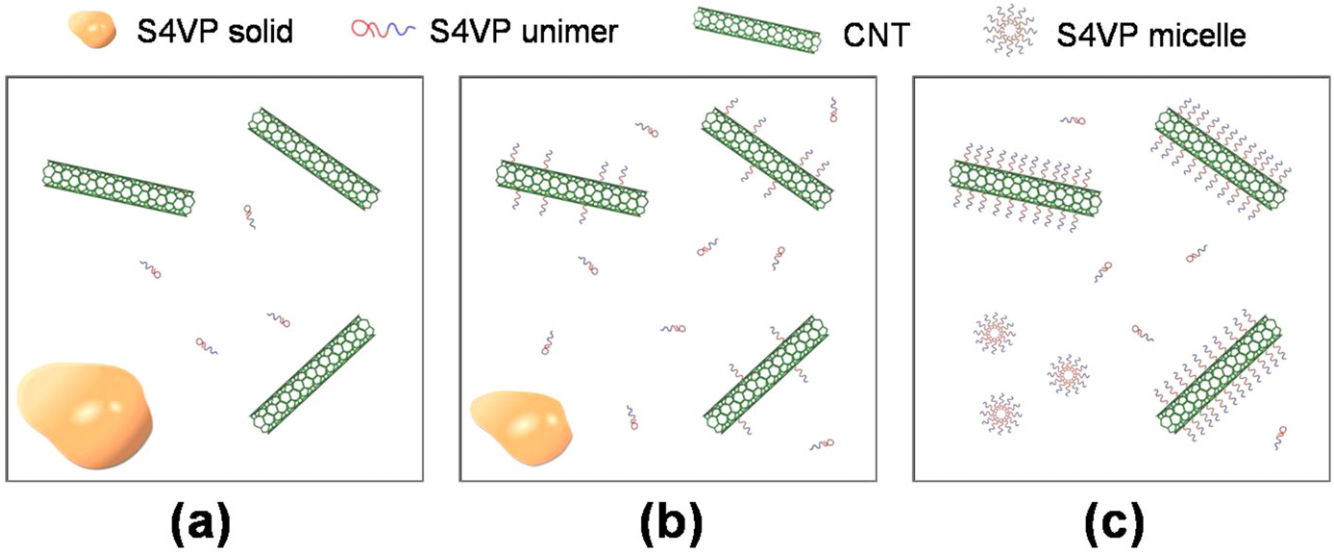

Figure 6. The schematic demonstration of the encapsulation process of CNTs by S4VP: (a) the progressive dissolution of as-received S4VP solids, forming S4VP unimers, (b) attaching of S4VP unimers on CNTs, and (c) formation of S4VP micelles after the completion of encapsulation of CNTs.

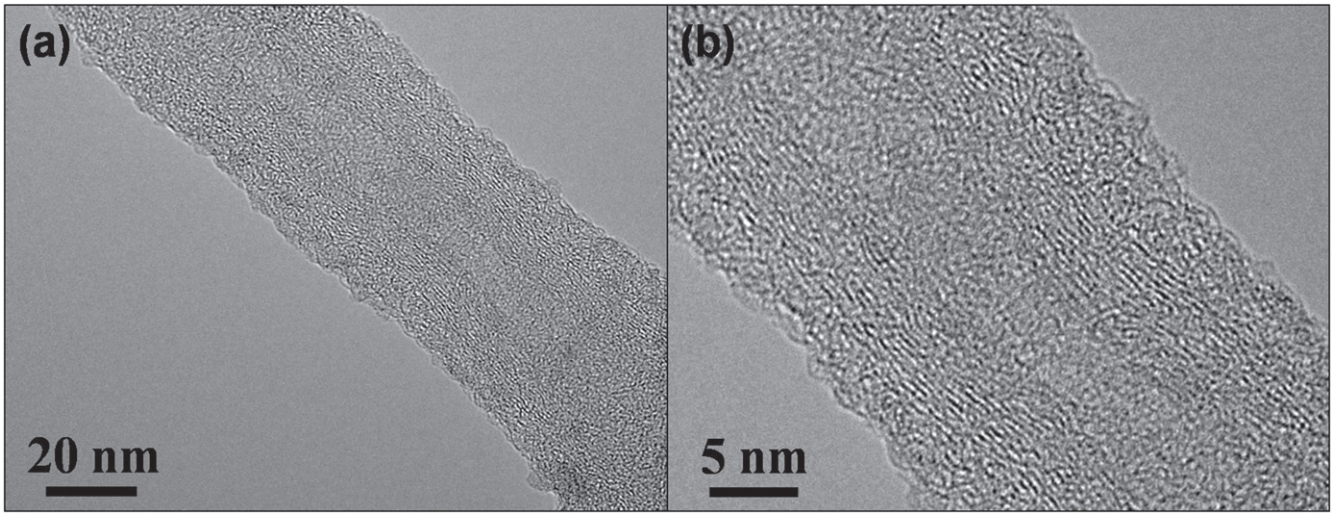

Figure 7. TEM images at different magnifications of CNTs obtained by mixing as-received CNTs and S4VP micellar solution in AA ($m_{BCP}/m_{CNT} = 2$) with sonication for 30 min followed by standing overnight.

~1.5 nm along the surface of the S4VP-coated CNTs (figures 8(b), (c)). The pristine CNTs possess a hydrophobic surface and are short of active groups for the chemical adsorption of ALD precursors. Consequently, TiO_2 nucleates on the surface defects of CNTs, forming isolated particulates in the following growth step [35]. For the S4VP-coated CNTs, their surfaces are predominantly covered with P4VP chains which contain chemically active pyridyl rings. As a result, ALD precursors can be readily adsorbed on the P4VP phases, leading to the conformal growth of TiO_2 layers. In addition, the infiltration of precursors into the subsurface of the polymer layer may also occur [36, 37] and as a result, there is no clear boundary between the polymer layer and the TiO_2 layer.

4. Conclusions

Amphiphilic block copolymers of PS and P4VP were uniformly coated on the surface of carbon nanotubes in solutions of AA. The copolymer was adhered to CNTs because of the π–π interaction between CNTs and benzene rings in PS blocks of the copolymer. The S4VP-coated CNTs possessed a lamellar structure with P4VP chains existing in the outermost layer, providing good dispersibility of CNTs in AA. The S4VP-coated CNTs remained stable in AA for long time even after dilution with other polar solvents, i.e. ethanol and water. Detailed studies revealed that the mass ratio between S4VP and CNTs needed to be larger than a threshold, which was determined to be ~1.5, to sufficiently stabilize CNTs in polar

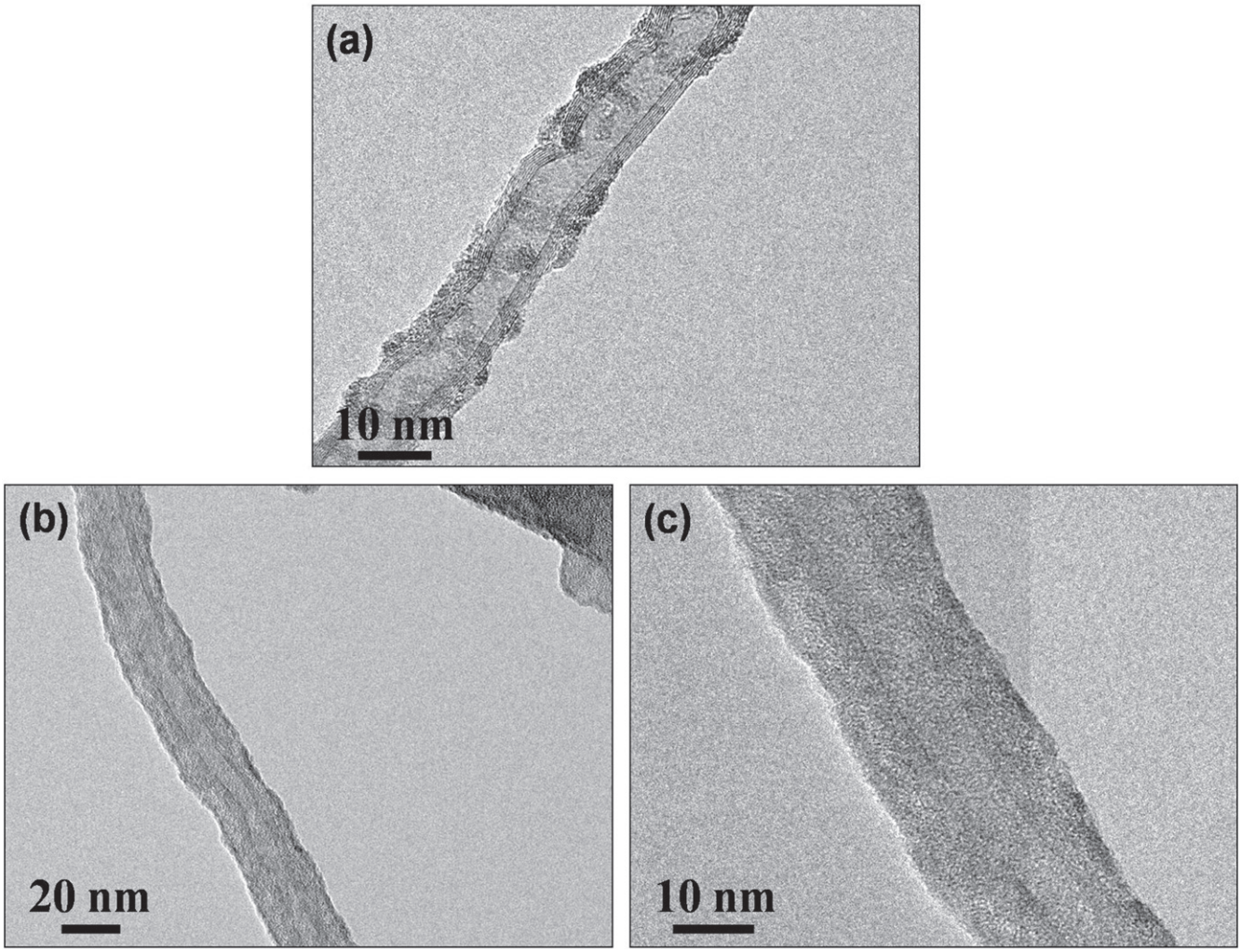

Figure 8. TEM images of the pristine (a) and S4VP-coated CNTs (b), (c) subjected to ALD deposition of TiO_2 for 100 cycles.

solvents and excessive S4VP would assemble into spherical micelles. The presence of P4VP chains on the surface of the CNTs provided an additional possibility for the functionalization and modification of CNTs. As an example, we demonstrated that a uniform thin layer of TiO_2 could be conformally ALD-deposited on the surface of the S4VP-coated CNTs while isolated, bump-like TiO_2 particulates were produced on the inert, pristine CNTs.

Acknowledgments

Financial support from the National Basic Research Program of China (2015CB655301), the Doctoral Program Foundation of Institutions of Higher Education of China (20123221110003), the Jiangsu Natural Science Funds for Distinguished Young Scholars (BK2012039), and the Project of Priority Academic Program Development of Jiangsu Higher Education Institutions (PAPD) is gratefully acknowledged.

References

[1] Qu L T, Dai L M, Stone M, Xia Z H and Wang Z L 2008 Carbon nanotube arrays with strong shear binding-on and easy normal lifting-off *Science* **322** 238–42
[2] Jorio A, Dresselhaus G and Dresselhaus M S 2007 *Carbon Nanotubes: Advanced Topics in the Synthesis, Structure, Properties and Applications* (Berlin: Springer)
[3] Foroughi J *et al* 2011 Torsional carbon nanotube artificial muscles *Science* **334** 494–7
[4] Sakellariou G, Priftis D and Baskaran D 2013 Surface-initiated polymerization from carbon nanotubes: strategies and perspectives *Chem. Soc. Rev.* **42** 677–704
[5] Bilalis P, Katsigiannopoulos D, Avgeropoulos A and Sakellariou G 2014 Non-covalent functionalization of carbon nanotubes with polymers *RSC Adv.* **4** 2911–34
[6] Moniruzzaman M and Winey K I 2006 Polymer nanocomposites containing carbon nanotubes *Macromolecules* **39** 5194–205
[7] Chen H and Ruckenstein E 2009 Nanoparticle aggregation in the presence of a block copolymer *J. Chem. Phys.* **131** 15384–410
[8] Chen H and Ruckenstein E 2010 Structure and particle aggregation in block copolymer-binary nanoparticle composites *Polymer* **51** 5869–82

[9] Chen H and Ruckenstein E 2014 Micellar structures in nanoparticle-multiblock copolymer complexes *Langmuir* **30** 3723–8

[10] Collison C J, Spencer S, Preske A, Palumbo C, Helenic A, Bailey R and Pellizzeri S 2010 A new model for quantifying the extent of interaction between soluble polyphenylene-vinylenes and single-walled carbon nanotubes in solvent dispersions *J. Phys. Chem.* B **114** 11002–9

[11] Giancane G, Ruland A, Sgobba V, Manno D, Serra A, Farinola G M, Omar O H, Guldi D M and Valli L 2010 Aligning single-walled carbon nanotubes by means of Langmuir-Blodgett film deposition: optical, morphological, and photo-electrochemical studies *Adv. Funct. Mater.* **20** 2481–8

[12] Pang X, Imin P, Zhitomirsky I and Adronov A 2010 Amperometric detection of glucose using a conjugated polyelectrolyte complex with single-walled carbon nanotubes *Macromolecules* **43** 10376–81

[13] Yang Z, Xue Z, Liao Y, Zhou X, Zhou J, Zhu J and Xie X 2013 Hierarchical hybrids of carbon nanotubes in amphiphilic poly (ethylene oxide)-block-polyaniline through a facile method: from smooth to thorny *Langmuir* **29** 3757–64

[14] Sluzarenko N, Heurtefeu B, Maugey M, Zakri C, Poulin P and Lecommandoux S 2006 Diblock copolymer stabilization of multi-wall carbon nanotubes in organic solvents and their use in composites *Carbon* **44** 3207–12

[15] Zou J, Liu L, Chen H, Khondaker S I, McCullough R D, Huo Q and Zhai L 2008 Dispersion of pristine carbon nanotubes using conjugated block copolymers *Adv. Mater.* **20** 2055–60

[16] Brown J J, Hall R A, Kladitis P E, George S M and Bright V M 2013 Molecular layer deposition on carbon nanotubes *ACS Nano* **7** 7812–23

[17] Chen Y, Zhang B, Gao Z, Chen C, Zhao S and Qin Y 2015 Functionalization of multiwalled carbon nanotubes with uniform polyurea coatings by molecular layer deposition *Carbon* **82** 470–8

[18] Shvartzman-Cohen R, Levi-Kalisman Y, Nativ-Roth E and Yerushalmi-Rozen R 2004 Generic approach for dispersing single-walled carbon nanotubes: the strength of a weak interaction *Langmuir* **20** 6085–8

[19] Shvartzman-Cohen R, Monje I, Florent M, Frydman V, Goldfarb D and Yerushalmi-Rozen R 2010 Self-assembly of amphiphilic block copolymers in dispersions of multiwalled carbon nanotubes as reported by spin probe electron paramagnetic resonance spectroscopy *Macromolecules* **43** 606–14

[20] Kang Y and Taton T A 2003 Micelle-encapsulated carbon nanotubes: a route to nanotube composites *J. Am. Chem. Soc.* **125** 5650–1

[21] Chen L, Wang H, Xu J, Shen X, Yao L, Zhu L, Zeng Z, Zhang H and Chen H 2011 Controlling reversible elastic deformation of carbon nanotube rings *J. Am. Chem. Soc.* **133** 9654–7

[22] Liu C, Chen G, Sun H, Xu J, Feng Y, Zhang Z, Wu T and Chen H 2011 Toroidal micelles of polystyrene-block-poly (acrylic acid) *Small* **7** 2721–6

[23] Arras M M L, Schillai C and Jandt K D 2014 Enveloping self-assembly of carbon nanotubes at copolymer micelle cores *Langmuir* **30** 14263–9

[24] Shin H-I, Min B G, Jeong W and Park C 2005 Amphiphilic block copolymer micelles: new dispersant for single wall carbon nanotubes *Macromol. Rapid Commun.* **26** 1451–7

[25] Sung J, Jo P S, Shin H, Huh J, Min B G, Kim D H and Park C 2008 Transparent, low-electric-resistance nanocomposites of self-assembled block copolymers and SWNTs *Adv. Mater.* **20** 1505–10

[26] Wang Y, Gosele U and Steinhart M 2008 Mesoporous block copolymer nanorods by swelling-induced morphology reconstruction *Nano Lett.* **8** 3548–53

[27] Gowd E B, Koga T, Endoh M K, Kumar K and Stamm M 2014 Pathways of cylindrical orientations in PS-b-P4VP diblock copolymer thin films upon solvent vapor annealing *Soft Matter* **10** 7753–61

[28] Muleja A A, Mbianda X Y, Krause R W and Pillay K 2012 Synthesis, characterization and thermal decomposition behaviour of triphenylphosphine-linked multiwalled carbon nanotubes *Carbon* **50** 2741–51

[29] Rasheed A, Dadmun M D, Ivanov I, Britt P F and Geohegan D B 2006 Improving dispersion of single-walled carbon nanotubes in a polymer matrix using specific interactions *Chem. Mater.* **18** 3513–22

[30] Jain S and Bates F S 2003 On the origins of morphological complexity in block copolymer surfactants *Science* **300** 460–4

[31] Yang Z, Wang Z, Yao X and Wang Y 2012 Water-dispersible, uniform nanospheres by heating-enabled micellization of amphiphilic block copolymers in polar solvents *Langmuir* **28** 3011–7

[32] Ma P-C, Siddiqui N A, Marom G and Kim J-K 2010 Dispersion and functionalization of carbon nanotubes for polymer-based nanocomposites: a review *Composites* A **41** 1345–67

[33] Hamilton W A, Smith G S, Alcantar N A, Majewski J, Toomey R G and Kuhl T L 2004 Determining the density profile of confined polymer brushes with neutron reflectivity *J. Polym. Sci.* B **42** 3290–301

[34] Zhang L F and Eisenberg A 1996 Multiple morphologies and characteristics of 'crew-cut' micelle-like aggregates of polystyrene-b-poly(acrylic acid) diblock copolymers in aqueous solutions *J. Am. Chem. Soc.* **118** 3168–81

[35] Cavanagh A S, Wilson C A, Weimer A W and George S M 2009 Atomic layer deposition on gram quantities of multi-walled carbon nanotubes *Nanotechnology* **20** 255602

[36] Lee S M, Pippel E, Gosele U, Dresbach C, Qin Y, Chandran C V, Brauniger T, Hause G and Knez M 2009 Greatly increased toughness of infiltrated spider silk *Science* **324** 488–92

[37] Peng Q, Tseng Y C, Darling S B and Elam J W 2010 Nanoscopic patterned materials with tunable dimensions via atomic layer deposition on block copolymers *Adv. Mater.* **22** 5129–33